

1 Damages induced by the 25 April 2015 Nepal earthquake in the
2 Tibetan border region of China and increased post-seismic
3 hazards

4

5 Zhonghai Wu ^{a*}, Patrick J. Barosh ^b, Guanghao Ha^a, Xin Yao^a, Yongqiang Xu ^c and Jie
6 Liu ^d

7

8 a Institute of Geomechanics, Chinese Academy of Geological Sciences, Beijing
9 100081, China

10 b P.J. Barosh and Associates, 103 Aaron Avenue, Bristol, RI 02809, USA and Visiting
11 Research Fellow, Chinese Academy of Geological Sciences, Beijing 100081
12 China

13 c China Institute of Geo-environment Monitoring, Beijing 100081, China

14 d College of Resource Environment and Tourism, Capital Normal University, Beijing
15 100048, China

16

17 **Abstract:** The seismic effects in Nyalam, Gyirong, Tingri and Dinggye counties along
18 the southern border of Tibet were investigated during 2-8 May, 2015, a week after the
19 great Nepal earthquake along the Main Himalaya Thrust. The intensity was VIII in the
20 region and reached IX at two towns on the Nepal border; resulting in the destruction of
21 2,700 buildings, seriously damaging over 40,000 others, while killing 27 people and
22 injuring 856 in this sparsely populated region. The main geologic effects in this steep
23 rugged region are collapses, landslides, rockfalls, and ground fissures; many of which
24 are reactivations of older land slips. These did great damage to the buildings, roads and
25 bridges in the region. Most of the effects are along four incised valleys which are
26 controlled by N-trending rifts and contain rivers that pass through the Himalaya
27 Mountains and flow into Nepal; at least two of the larger aftershocks occurred along the
28 normal faults. And, the damages are not related to the faulting of N-trending rifts but
29 distributed along the intensity of Nepal earthquake. Areas weakened by the earthquake
30 pose post-seismic hazards. Another main characteristic of damages is the recurrence of
31 the old landslide and rockfalls. In addition, there is an increased seismic hazard along
32 active N-trending grabens in southern Tibet due to the shift in stress resulting from the
33 thrust movement that caused the Nepal earthquake. NW trending right-lateral
34 strike-slip faults also may be susceptible to movement. The results of the findings are
35 incorporated in some principle recommendations for the repair and reconstruction after
36 the earthquake.

37

38 **Key Words:** Nepal earthquake, Himalaya Mountains, Seismic hazard, Post-seismic
39 hazardp

Corresponding author: Wu Zhong-hai, E-mail: wuzhonghai@geomech.ac.cn,

40

41 **1. Introduction**

42 On 25 April 2015 at 14:11:26 MGT+8 (Beijing Time), a great Ms 8.1 (Mw 7.8)
43 earthquake struck Nepal and adjacent regions killing more than 8,800 people and
44 injuring more than 23,000. The epicenter was near Pokhara 77 km northwest of the
45 capital of Kathmandu and the hypocenter was at a depth of 10-24 km. Many aftershocks
46 of magnitude 4.5 M_w or greater followed, of which a Ms 7.5 (Mw 7.3) aftershock
47 occurred after 17 days, on 12 May 2015 at 15:05. This epicenter was near the Chinese
48 border 77 km east-northeast of Kathmandu and the hypocenter was at a depth of 12-16
49 km.

50 The main earthquake occurred on the south slope of the Himalaya Mountains and
51 formed a 120-140 km long, about 80 km wide rupture zone with a dip-slip of 3.5-5.5 m,
52 which shows an expansion from west to east (USGS, 2015 a, b; IRIS, 2015). The
53 aftershock distribution, the focal mechanism solution and the source rupture inversion
54 suggest that the earthquake was a release of built-up strain along the Main Himalaya
55 Thrust fault zone and part of the ongoing process of the Indian Plate underthrusting the
56 Eurasian Plate (Fig. 1). This was the strongest seismic event since the 2005 Ms 7.8
57 Pakistan Kashmir earthquake, which also occurred along the Main Himalaya Thrust.
58 These earthquakes may indicate that the seismic activity along the thrust is entering a
59 new active phase.

60 The earthquake affected Nepal, northern India, Pakistan, Bhutan, and the southern
61 Tibet of China. Main damages characteristics have been reported in Nepal (Bijukchhen
62 et al., 2017; Yun et al., 2015). However, there is lack of damages investigation in China,
63 which is the focus of this paper. In China the tremors were felt in Xigazê and Lhasa to
64 the north and over 300,000 km², but were strongest in the China-Nepal border area
65 which is only about 40 km (Fig. 1, 2) from the epicenter (Table 1). Despite the great
66 loss of life in Nepal the disaster caused only 27 deaths, 856 injuries and 3 missing in
67 China, although the damage was extensive. About 30 thousand people were affected

68 and the direct economic loss is more than 33,000 million Yuan (RMB) (5.178 trillion
69 U.S. dollars). Fortunately, the border area has a low population density and the
70 earthquake occurred in the afternoon when many were outside, otherwise the casualty
71 and economic loss would have been much higher. Due to the rapid response of the local
72 governments the displaced people were soon resettled in southern Tibet.

73 An emergency seismic hazard investigation group of 12 people was organized by
74 the Ministry of Land and Resources to survey the hardest hit four counties of Nyalam,
75 Gyirong, Tingri and Dinggye during 2-8 May, a week after the main shock, in order to
76 quickly understand the earthquake effects and potential future threats to provide a basis
77 for the post-earthquake reconstruction. The group then held meetings with the local
78 governments to present their findings and recommendations. This paper is a brief
79 summary of the direct effects observed in the field and investigations into the delayed
80 effects that may cause as much damage.

81 **2. Seismic-Geological Setting**

82 The Tibetan Plateau is well known for its numerous E-W to NW, north-dipping
83 thrust faults (MHT) that facilitated its rise as the India plate collided and was thrust
84 beneath it. Most of the uplift occurred by the Miocene (Dewey et al, 1988; Wu et al.,
85 2008) and the majority of the thrust faults came to a stop as the movement evolved and
86 concentrated along fewer strike-slip faults, which remain very active and capable of
87 great earthquakes (Armijo et al., 1989; Fig. 1). However, thrusting remains dominant in
88 the collision zone at the south edge of Tibet south of the Himalaya Mountains with the
89 continued northward movement of India. Here the greatest activity occurs along the
90 very shallow north-dipping Main Himalaya Thrust, which gave rise to the Nepal
91 earthquake and has a long history of great earthquakes along its length (Fig. 1). Less
92 generally known are a series of nearly N-S-trending normal faults and grabens to the
93 north of the great thrust that complement some of the movement across it. These also
94 are capable of producing significant earthquakes, although they are much shorter in
95 length (Wu et al, 2011). This array of active faults plus a set of NW right-lateral

96 strike-slip faults, which may aid extension, constitute the seismic framework of the
97 region.

98 The China-Nepal border region is located on the south slope of the Himalaya
99 Mountains close to the Main Himalaya Thrust and contains many active normal faults
100 that control the transverse valleys that lead into Nepal. The high, rugged, steep
101 topography and the well-developed incised river valleys in this region further amplify
102 the destruction caused by earthquakes. Therefore, it is not strange that southern Tibet
103 was greatly affected by the Nepal earthquake.

104 **3. Methods and data**

105 The intensity was evaluated using the Chinese seismic intensity scale (GB/T
106 17742-2008) (CSIS), which is a revised national standard implemented in 2009, that
107 has 12 degrees of intensity (GB/T, 2008). This was modified from the GEOFIAN
108 (Medvedev) scale, that in turn was adapted from the Modified Mercalli scale and is
109 closely aligned with it, except in the lower units (Barosh, 1969) and is approximately
110 the same in the higher units reported on herein. The latest CSIS scale revision added an
111 additional building type for evaluation in reflecting newer construction in the country.

112 A broad region of southern Tibet was affected by the earthquake, but the sparse
113 population and difficult terrain did not permit defining of the felt area well. Most
114 isoseismics for the lower intensities were compiled by the China Earthquake
115 Administration, which made a quick, overall survey of towns in order to assess the
116 damage (Fig. 1). However, a detailed field survey, reported below, was made in the
117 region most affected. The principal effects of the earthquakes are the damage suffered
118 by structures, highways and bridges and the landslides, collapses and rockfalls. The
119 landslips caused much of the damage to the construction. Overall 2,699 houses and one
120 temple were destroyed, 39,981 houses and 242 temples seriously damaged, and about
121 2,600 km of main highways, 263 bridges, and a part of the communication, power and
122 water facilities were damaged to some degree in southern Tibet as reported by the
123 China Earthquake Administration. In the region more closely studied in the field the

124 damage and seismic intensity were evaluated at 29 sites in 10 affected counties (Fig. 2,
125 and Table 1).

126 **4. Results**

127 **4.1. Damage features and seismic intensity**

128 Landslides, rockfalls and collapses are common widespread occurrences during
129 large earthquakes in the mountainous regions of Tibet. The Nepal earthquake was no
130 exception, even though there was no nearby surface fault offset. The 2008 Ms 8.0
131 Wenchuan earthquake and its aftershocks at the eastern edge of Tibet produced
132 hundreds of thousands of such landslips (Wang and Han, 2010; Tang et al., 2011; Yang
133 et al., 2015). They caused major destruction and casualties, in addition to blocking river
134 valleys and forming reservoirs that threatened downstream communities. It was only a
135 massive emergency effort by the government that prevented additional major
136 calamities. Several small dams were formed by the Nepal earthquake, but no large ones
137 that needed an emergency excavation, although the threat remains.

138 The perception of the earthquake, damage to buildings of different material and
139 structure, and surface effects show obvious differences as recorded at the different
140 levels of intensity. Only a few people in a room might have felt the earthquake in Lhasa
141 at intensity III, whereas, to most of the people both inside and outside of buildings in
142 Xigazê city the earthquake was obvious and demonstrates an intensity IV and strong
143 damage indicates approximately intensity IX at the Nepal border. The increasing and
144 varying degrees of damage of buildings and disruptions of the surface in the VI to IX
145 intensity zones were reviewed in the field in southern Tibet nearer Nepal (Table 1). The
146 intensity described herein is a composite of both the main shock and the large after
147 shock. This may have caused an enhancement of the ratings if they were for the main
148 shock alone, because some structures weakened by it were further damaged or
149 destroyed by the large aftershock.

150 Of the four counties investigated, Nyalam County is located on the south slope of
151 the Himalaya Mountains, whereas Gyirong, Tingri, and Dinggye Counties are located

152 north of the mountains (for their seismic intensities, see Table 1). The main effects and
153 economic losses are concentrated in Nyalam, Tingri, and Gyirong Counties (Fig. 2)
154 where about 80% of the houses were completely destroyed or damaged to a large extent
155 (Figs. 3, 4). The damage is heaviest in the towns of Zhangmu in Nyalam County; Jilong
156 and Sale in Gyirong County, and Rongxia in Gyirong County (Fig. 5). Moreover, the
157 highways and communications to the towns of Zhangmu, Tingri, and Resuo Bridge as
158 well as connections to Zhangmu, Tingri, Chentang and others in Nyalam County were
159 greatly damaged and broken.

160 The Chinese intensity scale considers the varying effects on different building
161 types and this usually improves the reliability of the general intensity assignment, but
162 locally it may lead to assigning different values, if there is a greater variation in damage
163 than usual between types. This could be the case in these areas where the effects appear
164 to reach either intensity VIII or IX depending on the type of structure used to assign
165 intensity. The apparent highest intensity, IX, from destruction, that equaled some parts
166 of Kathmandu, for older self-built stone masonry or adobe structures with poor seismic
167 resistance, whereas for the newly built cement-bonded stone, brick or concrete
168 structures it was no more than intensity VIII and the rating lies between (Figs. 3 and 4).
169 For example, in Jifu Village about 2.4 km south of Jilong, all the houses built of stone
170 block masonry were almost completely destroyed, whereas most newly built ones of
171 cement-bonded stone or brick are still standing with only minor cracks in the walls (Fig.
172 4c-d), and the same variation also is seen at the Sale Town Primary School (Fig. 4e).
173 The inhabitants of this area had to be quickly moved to temporary settlements (Fig. 4b).
174 Perhaps some poorer buildings weakened by the first earthquake were collapsed by the
175 second one or the newer buildings had more seismic resistance than realized. Some
176 undetected ground slippage at a few locations throughout the region also may have
177 augmented the effects to a slight degree.

178 The E-W elongation of the intensity pattern (Fig. 2, Table 1) shows at least twice
179 the rate of attenuation northward towards the Himalaya Mountains than in an E or W
180 direction. This can be attributed to the absorption of the seismic energy by the
181 E-W-trending fault structure and lithologic units of the great Himalaya Mountain block,

182 plus a contribution from the E-W spread of the earthquakes and aftershocks.

183 The geologic effects caused by the Nepal earthquake are mainly landslides, terrace
184 and loose material collapses and debris flows, rockfalls, and ground fissures that were
185 studied in detail at 33 sites in four towns in Nyalam, Gyirong, Tingri and Dinggye
186 Counties (Figs. 2, 6). These vary with the intensity, amount of rock weakened by
187 previous movement, steepness of slope and lithology. These landslips diminish in
188 number and size northward from the Nepalese border with the decrease in intensity. In
189 the areas approaching intensity IX landslides and collapses are widespread and include
190 some large landslides; in the area encompassing intensity VIII small collapses and
191 landslides were common, but large landslides are rare; intensity VII areas contain some
192 small landslides, collapses and rockfalls along valley slopes and roadcuts; whereas in
193 the area of intensity VI small collapses and landslides are rare and a small amount of
194 rockfalls occurred near roadcuts.

195 These damages have the following characteristics:

196 (1) They are all disrupted slides, as classified by Varnes (1978; updated by Hungr
197 et al., 2014), with a loss of internal cohesion.

198 (2) They occur most densely along four incised river valleys, which are controlled
199 by N-S-trending rifts that pass through the Himalaya Mountains and enter into Nepal
200 (Fig. 2). The four valleys, successively from west to east, are: the Gyirong Zangbo
201 valley that follows the Gyirong Graben and extends southwards (Figs. 5b and 6e), the
202 Boqu River valley that follows the Nyalam Graben and passes through Zhangmu and
203 connects to the Sunkoxi River valley in Nepal (Figs. 5a and 6a); the Rongxiaqu valley
204 that follows the southwest side of the Kong Co-Gangga Graben to pass through
205 Rongxia and descend to the Sunkoxi River valley in Nepal (Fig. 5c) and, the Pengqu
206 River valley, controlled by the Paiku Co Rift, that crosses the Kung Co-Gangga Graben
207 and the Pengqu Graben southwards and passes through Chentang to connect to the
208 Arun River in Nepal (Fig. 5d). The topographic relief in these valleys is generally about
209 2,000-3,000 m, which is very favorable for various landslips during seismic events.
210 Furthermore, there is an overall tendency for the number and size of collapses,
211 landslides, and rockfalls to increase towards Nepal along these valleys.

212 Remotely-sensed images issued by Google Earth after the earthquake show that the
213 Gyirong Zangbo and the Buqu River valleys contain the maximum density and scale of
214 collapses and landslides (Figs. 5a, 5b, and 6a-6h).

215 Moreover, some dammed lakes due to the collapsed rock and soil can be seen in
216 these valleys of Nepal. For example, in the Gyirong Zangbo valley, a 0.07 km² dammed
217 lake and a 0.04 km² dammed lake occur about 2.5 km north of and about 7.3 km
218 southwest of Dhunche Village, respectively, and in the Boqu River valley, a 0.24 km²
219 dammed lake occurs on the north side of Dabi Village.

220 (3) Damages occur often in weak, soft geologic material and unstable geomorphic
221 positions: joint or fault-formed, high, steep bedrock cliffs and slopes (Figs. 6b and 6e);
222 high, steep slopes of loose Quaternary sediment forming river terraces, proluvial fans,
223 and benches (Figs. 6d and 6f) and; unstable slopes and highway road cuts (Figs. 6g and
224 6h). These landslides mostly occur on slopes steeper than 35-45 degrees.

225 (4) Most of large ground fissures are associated with collapses and landslides. They
226 either occur on the displaced masses or around their edges and only a few such fissures
227 occur on surface of loose sediments (Fig. 8).

228 These rock and soil slips caused the most serious casualties and damage. The worst
229 collapse found occurred in Disigang Village about 0.8 km southwest of Zhangmu
230 where about 0.016 km³ of debris destroyed four or five buildings and killed seven
231 people (Figs. 4a, 6b and 6c). The largest landslide found occurred about 1.3 km
232 southwest of Chongse Village near Jilong where about 2,700,000 m³ of material
233 blocked the main highway from Jilong to Gyirong Port (Fig. 6e). In addition, 27 small
234 landslides and collapses occurred along the 14 km length of highway stretching from
235 this landslide to Gyirong Port.

236 **4.2 Recurrence of seismo-geological hazards**

237 An important discovery was that the earthquake induced landslide and collapse
238 generally occurred where previous ones had taken place and correlated in size with the
239 previous ones. This apparently reflects the effects of ancient earthquakes and provides
240 new evidence for paleo-seismicity both in location and size. More significantly this

241 demonstrates the areas of ancient landslide and collapse indicate the potential areas of
242 danger from further landslips from torrential rains and future earthquakes; important
243 considerations in seismic risk evaluation and the post-earthquake reconstruction
244 process.

245 The collapses and landslides commonly result from reactivation of older ones and
246 similar effects produced by historic earthquakes occurred near the same position as in
247 this earthquake. Such features are notable on both banks of the Boqu River near
248 Zhangmu (Figs. 7a and 7b). At Disigang Village of Zhangmu, for example, a house
249 built on the side of a large rock brought down previously was destroyed by a new large
250 rockfall (Fig. 6c). This is a warning that reconstruction after the earthquake, not only
251 should avoid as far as possible potential new hazards, but at the same time be aware of
252 previous ones and make a comprehensive assessment of their stability.

253 The specific structural damage is usually related to the material and type of
254 building construction in these areas where the heaviest destruction occurred near the
255 Nepal border. In this region of few trees most of the houses are of simple stone and
256 adobe construction and these fared poorly during the earthquake; with the majority
257 being destroyed near Nepal (Figs. 3b, 3d, 3e, 4c). Houses with cement bonded stone or
258 brick construction survived much better (Figs. 3a, 4d) and those of good brick or
259 reinforced concrete construction suffered the least (Figs. 3c, 4f) and provided a contrast
260 with those of poorer materials (Figs. 3a, 4e).

261 **4.3 Post-seismic Increased Potential Geological Hazard**

262 The Nepal earthquake has left many potential dangers in its wake in this region and
263 nearby seismically active areas in southern Tibet that do not fit into an intensity scale
264 yet are a consequence of the earthquake and pose a serious hazard that might create
265 even greater damage and casualties than the immediate effects. The delayed effects in
266 southern Tibet are the consequences of earthquake-loosened landslides and weakened
267 rock that may fall due to aftershocks and torrential storms and from secondary
268 earthquakes due to changes in the stress field resulting from the Nepal earthquakes.

269 Rock, terrace material and previous landslides loosened by the earthquake, but still

270 in place may fail with small aftershocks and torrential rains, which further weaken the
271 material and add weight. Such an increase in secondary landslips during rainy seasons
272 following earthquakes has been noted previously and is becoming a recognized hazard.
273 Increased rainfall-triggered landslide activity above normal rates have been observed
274 after several large earthquakes; two of which occurred in similar terrane to the east and
275 west (Hovius et al., 2011; Saba et al., 2010; Tang et al., 2011; Dadson et al., 2004). Rain
276 may even be a factor during an earthquake. Data in New Zealand suggest that
277 earthquakes that occur during wetter months trigger more landslides than those during
278 drier periods; although a clear relationship between rainfall-induced pore pressure and
279 earthquake-induced landslide triggering has not been shown (Dellow and Hancox,
280 2006; Parker et al., 2015). When the typhoon Toraji hit Taiwan following the 2005 Mw
281 7.6 Chi-Chi earthquake, 30,000 more landslides occurred with many being reactivated
282 ones triggered by the earthquake, although 80% of the Toraji landslides occurred in
283 areas that had not failed during the earthquake (Dadson et al., 2004). The proportion of
284 surface area disturbed by the landslides increased towards the active fault suggesting
285 that even in areas that underwent no landslips during the earthquake the substrate was
286 preconditioned to fail through loss of cohesion and frictional strength of hill slope rock
287 mass caused by the strong seismic motion (Dadson et al., 2004).

288 A similar general weakening of rock strength was deduced in the mountainous
289 region of South Island, New Zealand where to test the possible influence of previous
290 earthquakes in preconditioning the ground for landsliding, the areas of overlap of high
291 intensity of similar strong, >Mw 7, 1929 and 1968 earthquakes were compared (Parker
292 et al., 2015). Many landslides produced in 1968 were reactivations or enlargements of
293 ones that failed in 1929, but others were not, although there was a higher degree of
294 failure in the overlapped area than could be easily explained in considering all the
295 factors normally involved in landslip. These observations suggested that hill slopes
296 may retain damage from past earthquakes, which makes them more susceptible to
297 failure in future triggering events, and this had influenced the behavior of the landscape
298 in the 1968 earthquake. It was further suggested that the damage legacy of large
299 earthquakes may persist in parts of the landscape for much longer than the observed

300 less than 10 year periods of post-seismic landslide activity and sediment evacuation.

301 Similarly, data from the 2010 Mw 7.1 Canterbury – 2011 Ms 6.3 Christchurch
302 earthquake sequence reveal landslide triggering at lower ground accelerations
303 following the February 2011 earthquake, which caused cracks to develop in hill slopes
304 that subsequently failed in later earthquakes in the sequence (Massey et al., 2014a,
305 2014b; Parker et al., 2015).

306 This general loosening of rock by ground motion also occurred at the Nevada Test
307 Site where deep underground nuclear explosions, similar to shallow earthquakes,
308 caused widespread movement along joints within the overlying bedrock (Barosh, 1968).
309 Some fractures were propagated upward through 610 m of alluvium to demonstrate
310 how even this soft material was weakened further.

311 The progressive brittle damage accumulation in hill slope materials may lead to
312 permanent slope displacement that results in cracking and dilation of the mass, which
313 makes them more susceptible to failure (Petley et al., 2005; Nara et al., 2011; Bagde
314 and Petroš, 2009; Li et al., 1992b; Parker et al., 2015). Whether or not a hill slope fails
315 in response to an earthquake thus, becomes a function of both a current event and the
316 history of damage accumulated from previous events (Parker et al., 2015).

317 These later landslides pose all of the same dangers as those occurring during the
318 initial earthquake and also may cause damming of rivers to create dangerous reservoirs
319 that can fail with devastating effects.

320 The landslips also increase the hazard from flooding in the disturbed region. They
321 contribute debris to valleys to widen them and raise river beds that greatly raises the
322 flood danger as has happened in the region of the Wenchuan earthquake since 2008
323 (Yang et al., 2015). This is a problem that needs to be recognized in post-earthquake
324 reconstruction.

325 Such consequences from earthquakes are long lasting. It is estimated to have taken
326 three years for the Kashmir earthquake region to recover; six for the Chi-chi earthquake;
327 over seven for the Wenchuan earthquake and even longer for others (Saba et al., 2010;
328 Yang et al., 2015; Dadson et al., 2004).

329 There is a worry of additional landslides and rock falls after the Nepal earthquake,

330 especially of large ones, that might block river valleys and impound water. Indeed, both
331 the number and range of collapse and rock fall has clearly increased in this year's rainy
332 season following the earthquake. Zhou (2015) noted that before the earthquake
333 collapses and rockfalls only occurred on steep hill slopes on both sides of the Bo Qu
334 River north of Zhangmu Town, but now take place along the entire highway in this area.
335 He reports that the increased hazard has caused many road closures and damaged
336 vehicles, but no casualties as yet, because the town was evacuated after the earthquake.
337 The increased hazards are mainly distributed nearby along the highway between
338 Nyalam to Zhangmu where eighteen major landslide groups have been identified after
339 the earthquake by the National Disaster Reduction Center of the Ministry of Civil
340 Affairs using high resolution remote sensing images. Such an increase in the number of
341 slides should be widespread in several major valleys of southern Tibet, but relatively
342 few have been reported due to scarce personnel and poor transportation and
343 communication.

344 Unstable masses found to date are: the reactivated landslide group at Zhangmu,
345 collapse of the upper edge of the Sale Village landslide in Sale, potential failure of the
346 dangerous rock mass at the Rongxia Primary School, and instability of the old Natang
347 Village landslide and its upper edge at Chentang Town.

348 All of Zhangmu is located on a group of old landslides (Figs. 4a, 7a and 7b).
349 Discontinuous tension fissures, which are tens to hundreds of meters long, about 10 cm
350 wide and 2 to 4 m deep, were found at its upper edge and on its sides after the
351 earthquake (Figs. 8a and 8b). These fissures indicate the possibility of the failure of the
352 entire landslide group.

353 The Sale Village landslide, which resulted from the earthquake, on the slope along
354 the highway from Sale Village to Seqiong Village (Fig. 5b). It is nearly 600,000 m³ in
355 volume and its fall blocked the road. Large tension fissures at its upper edge indicate a
356 danger of further slippage (Fig. 8c).

357 The dangerous rock mass at the Rongxia Village Primary School occupies a
358 convex portion of the cliff behind the school and appears unstable (Figs. 5c and 8d). A
359 rockfall occurred here during the earthquake, but the fall appears to have been

360 incomplete and left a cliff that lacks stability and is susceptible to further rockfall.

361 Natang Village near Chentang is located at the front, lower edge of an old landslide,
362 which is about 420 m long and 230 m wide, and consists of about 1,200,000 m³ (Figs.
363 5d and 8e). The steep wall at its upper edge appears as two large dangerous rock blocks
364 which are about 60,000 m³ in volume and a 1.7 m wide preexisted crack occurs between
365 the unstable rock blocks and the bedrock (Fig. 8f). The earthquake caused a partial
366 rockfall and demonstrates the dangerous instability of the mass that might come down
367 easily.

368 The danger of post-seismic debris flows also must be stressed, although these were
369 rare for this earthquake in the southern Tibet region; they were a serious problem in the
370 Wenchuan earthquake (Cui et al., 2010; Tang et al, 2011). There is, however, a
371 considerable amount of loose debris accumulated in mountain valleys and gullies that
372 could provide material for further debris flows, especially on the south slope of the
373 Himalaya Mountains. Rainfall, which provides excessive water to lubricate land slips
374 and adds weight to a loose mass, is a key factor in inducing post-seismic debris flows as
375 well as triggering landslides and rockfalls. There is a large difference in rainfall
376 between the south and north slopes of the Himalaya Mountains. The annual average
377 rainfall at Zhangmu on the south slope is up to 2,556.4 mm/a, whereas the annual
378 average rainfall in Jilong and the seat of Nyalam County on the north slope is only
379 880.3 mm/a and 654.0 mm/a, respectively. The rainfall on the south slope is
380 concentrated in the Indian Ocean summer monsoon season and induced debris flows
381 were already being reported in Nepal at the beginning of June. The several incised
382 valleys in the south mentioned above are sites of potentially dangerous post-seismic
383 debris flows in Tibet particularly in the three deeply incised valleys leading toward
384 Nepal that have a high potential for flows that could dam the rivers to form dangerous
385 lakes. These valleys, from west to east, are: The Gyirong Zangbo River in the upper
386 basin of the Trisuli River, the Boqu River and the Rongxiaqu River in the upper basin of
387 the Sunkoxi River (Fig. 2). Another danger spot is in the Dianchang gully on the south
388 side of Zhangmu (Figs. 5a and 7a) where considerable loose debris is in a very unstable
389 state.

390 **5. Discussion**

391 **5.1 Pattern of damages**

392 The Nepal earthquake was felt over a wide region of southern Tibet. Fortunately,
393 few casualties occurred, because of the sparse population, but there was extensive
394 damage due to the presence of many poorly built stone and adobe buildings and the
395 impact of landslides, collapses and rockfalls in this steep mountainous region of high
396 relief that is similar in the Nepal region (Zekkos et al., 2017); the intensity near the
397 Nepal border approached IX. The intensity distribution showed that the attenuation rate
398 northward was more than twice that in either eastward or westward directions due to the
399 absorption of energy by the major E-W-trending structure of the region and the trend of
400 the seismic activity in the epicentral area. The intensity survey demonstrated a very
401 wide difference in seismic performance between these poorly built buildings and
402 well-built brick and concrete ones. In addition to the immediate damage shown by the
403 intensity, there are the delayed effects of further dangerous land movement and an
404 increased potential for a significant earthquake over the next several years; all of which
405 are important in consideration of the seismic hazard in the region and post-earthquake
406 reconstruction.

407 The numerous landslides, collapses and rockfalls occurred on slopes steeper than
408 35-45 degrees and usually at locations where previous one took place. This apparently
409 reflects the effects of ancient earthquakes and provides new evidence for
410 paleo-seismicity. The presence of large landslides, which either did not fail or only
411 partially so, also suggests that larger earthquakes affected this region in the past. These
412 sites of ancient and modern slips mark the hazardous areas in future earthquakes; an
413 important consideration in seismic risk evaluation and the post- earthquake
414 reconstruction process.

415 The Nepal earthquake both changed and brought out features that enhance the
416 seismic hazard in the near and long term. The principal geologic dangers emanate from
417 landslides, collapses and rockfalls in this steep terrane from ones loosened or only

418 partially failed immediately or new ones from ground weakened by the general ground
419 shaking of the earthquake. These will be more common in the next three to six years or
420 so as a delayed effect of the earthquake, especially in seasons of heavy rainfall. All of
421 the areas of older landslips, whether or not they reactivated in this earthquake, are
422 susceptible to reactivation and are particularly dangerous. In recent years it has been
423 discovered that ground motion from large earthquakes results in weakened
424 cohesiveness of the ground and causes more abundant landslips subsequently. These
425 may clog valleys to form dangerous reservoirs. Such an increase in landslips has
426 already been note in the study area this past summer.

427 Both the landslips during an earthquake and the delayed ones contribute debris to
428 the river valleys to widened them and raise riverbeds to create conditions for flooding.
429 This can destroy additional buildings and endanger bridges as in the area of the
430 Wenchuan earthquake (Yang et al., 2015).

431 Following these characteristics, we should focus three circumstances in the
432 assessments of seismic geological hazards (mainly refers to collapse, landslips and
433 rockfall here) within the many strong earthquakes and high relief area:

- 434 (1) steep slopes formed by loose bodies, such as thick alluvial and residual deposits,
435 in deep valleys;
- 436 (2) places with multiple periods of landslides, collapses and rockfalls;
- 437 (3) the revival possibility of known landslides and collapses in future earthquakes.

438 **5.2 Relationship between MHT and N-trending rifts**

439 The Nepal earthquake has likely set the stage for another forceful nearby
440 earthquake that can be considered a delayed effect. The release of energy in a great
441 earthquake such as the Nepal earthquake may shift the strain in the adjacent regions
442 where other earthquakes may then occur, such as the strong earthquakes that occurred
443 in Tibet following the Ms 8.0 Wenchuan earthquake (Wu et al, 2011). The seismic
444 history of southern border of Tibet appears to bear this out. Large earthquakes along the
445 south margin on the Main Frontal Thrust of the Main Himalayan Thrust are followed by

446 ones along the N-S-trending normal faults in the region to the north (Fig. 1). There now
447 is an increased concern that a significant earthquake may occur along the normal faults
448 in the region based on this past history

449 Southern Tibet is an earthquake-prone region with long E-W-trending active thrust
450 faults such as caused the Nepal Earthquake; less well known are the important active
451 normal faults and grabens just to the north (Figs. 1 and 2). These normal faults form at
452 least eight nearly N-S-trending rifts across southern Tibet. Geological estimates and
453 GPS data show that the E-W extension rates cross the rifts were 10-13 mm/a during the
454 Quaternary and Holocene (Armijo et al., 1986; Chen et al., 2004). Such rates are close
455 to the Holocene slip rate of 21 ± 1.5 mm/yr along the Main Frontal Thrust of the Main
456 Himalaya Thrust (Lavé and Avouac, 2000) and to the recent GPS-based shortening rate
457 of 10-19 mm/yr across the Himalaya orogenic belt (Larson et al., 1999; Jouanne, et al.,
458 1999; Zhang et al., 2004; Bettinelli et al., 2006). There thus, appears to be a close
459 kinematic connection between the thrusting on the Main Himalaya Thrust and the
460 nearly N-S-trending normal faulting in the southern Tibet region as indicated by the
461 historic seismicity (Armijo et al, 1989; Molnar and Lyon-Caen, 1989).

462 Often within a short time interval of about one to 10 years after great earthquakes
463 on the Main Himalaya Thrust, strong earthquakes occur on the N-S-trending normal
464 faults in the southern Tibet region (Fig. 9). For example, the great Kashmir earthquake
465 of 1400 was followed by a M 8.0 earthquake in the Damxung-Yangbajain sector of the
466 northern Yadong-Gulu Rift in 1411; a M 8.1 earthquake in the western part of Nepal in
467 1803 was followed by a M 7.5 earthquake in the southern sector of the Cona-Oiga Rift
468 in 1806, and the M 7.8 Kashmir earthquake of 1905 was followed by a M 7.5
469 earthquake at Sangri in the northern sector of the Cona-Oiga Rift in 1915. Similarly,
470 after the M 8.1 1934 Nepal earthquake, a M 7.0 earthquake in the same year occurred in
471 the N-S-trending Gomang Co graben in northeastern Xainza County and after the 1950
472 M 8.6 China-Indian border earthquake, a M 7.5 earthquake occurred in 1952 in the
473 northern sector of the Yadong-Gulu Rift in Nagqu County.

474 Another delayed effect of the earthquake is the enhanced seismic hazard due to the
475 release in energy and the shift in strain, based on the past seismic history. The Nepal

476 earthquake emphasizes the close relation between the seismic activity and the dynamics
477 in the nearly east-west stretch of deformation along the Himalaya foothills and the
478 controlling activity along the Main Himalaya Thrust, which triggered the Nepal
479 earthquake. Extensional forces about perpendicular to the active thrust have a history of
480 resulting in a nearby significant normal fault earthquake following thrust movement
481 within the subsequent 10 years that results in further destruction and fatalities. Some
482 normal fault activity has indeed been noted in the aftershocks of the Nepal earthquake,
483 but not nearly enough to release the expected strain.

484 On the first and second day after the 2015 Nepal earthquake a Mw 5.4 earthquake
485 occurred in Nyalam County and a Ms 5.9 earthquake in Tingri County, respectively.
486 Both are nearly N-S-trending normal faulting-type earthquakes: the former occurred in
487 the Nyalam-Coqên Rift and the latter at the southern end of the Xainza-Dinggye Rift.
488 However, these movements are unlikely to have released all the built up extensional
489 force. Recently, Elliott et al. (2010) found from the InSAR and body wave
490 seismological images of normal faulting earthquakes that the extension rate due to the
491 contribution of the seismic energy released through normal faulting for the past 43
492 years in the southern Tibet region is 3-4 mm/a, which is only equivalent to 15-20% of
493 the extension rate obtained by GPS measurements. This suggests that there still is about
494 80% of the energy due to extension to be released, possibly as near-future seismic
495 activity.

496 The extension also may affect a set of NW-trending right-lateral strike-slip fault
497 zones that have significant activity in the southern Tibet region. These are from west to
498 east: The Karakorum fault zone, the Gyaring Co fault zone, and the Bengcuo fault zone
499 (Fig. 1). Their Quaternary strike-slip rate may reach 10-20 mm/a (Armijo et al., 1989;
500 Chevalier et al., 2005). Such faults with high strike-slip rates also can play an important
501 role in adjusting of the nearly E-W extensional deformation in the area. For example, a
502 M 8.0 earthquake in southwestern Nagqu in 1951, which occurred along the
503 NW-trending Bengcuo fault zone, followed the 1950 M 8.6 Zayü earthquake of eastern
504 Tibet that is known in India as Assam earthquake.

505 Based on past experience, the southern Tibetan region in the vicinity of the Nepal

506 earthquake is likely to have a normal fault earthquake within the next 10 years.

507 **5.3 Suggestions for regional earthquake prevention and disaster mitigation**

508 This investigation is preliminary and generalized, but tentative recommendations
509 can be issued to guide reconstruction in the region.

510 First, southern Tibet is a region with remarkable historical seismicity where
511 earthquakes and their effects cannot effectively be forecast, but a reevaluation of the
512 earthquake hazards should be made as soon as possible to indicate the potential dangers
513 noted in this survey.

514 Second, the relocation and reconstruction of damaged residential areas needs to
515 consider the potential dangers of post-seismic hazards and stability of previous
516 seismically induced geologic effects. Areas of ancient landslides, collapse and rockfall,
517 in particular need to be mapped and avoided, specially for schools, hospital, utilities
518 and vital government buildings and, where impossible, roads and bridges. Bridges
519 might be rebuilt higher in valleys where riverbeds may be raised and the flood danger
520 enhanced due to increased debris flow from the displaced material. And for the same
521 reason selection of building sites in valleys must be chosen with care. A wide selection
522 for new, safer sites for construction should be provided in the vast southern Tibetan
523 region with its very low population density.

524 Third, in the repair and reconstruction of buildings, new anti-seismic construction
525 codes must be adopted. The replacement of poorly built stone and adobe building by more
526 seismic resistant brick and concrete ones should be given a high priority.

527 Fourth, over the next 10 years there should be heightened awareness and
528 preparations for a possible earthquake in one of the grabens of southern Tibet.

529 Finally, although more detailed seismic-geological study is, of course, necessary,
530 the greater urgency should be directed at the construction of better anti-seismic
531 buildings and facilities in areas away from potential geological hazards that may be
532 triggered by earthquakes.

533

534 **6. Conclusions**

535 (1) Damages caused by Nepal earthquake in Tibet vary with the intensity, amount
536 of rock weakened by previous movement, steepness of slope and lithology. And the
537 damages show directional features mainly developed in the N-trending rifts in southern
538 Tibet. However, the damages weren't related to the faulting of N-trending rifts.

539 (2) The earthquake induced landslide and collapse generally occurred where
540 previous ones had taken place and correlated in size with the previous ones. Therefore,
541 the areas of ancient landslide and collapse indicate the potential areas of danger from
542 further landslips from torrential rains and future earthquakes.

543 (3) The damages directional features, paleo-earthquakes and deformational rate
544 also suggest that the E-W extensional deformation in southern Tibet is closely
545 associated with the Himalaya thrust fault. Then, the activity of MHT could trigger the
546 active faulting of N-trending rifts.

547

548 **ACKNOWLEDGEMENTS**

549 This work was supported by National Natural Science Foundation of China (No.
550 41571013 and 41171009). We would like to thank Professor Tingshan Tian and Jietang
551 Lu of the China Institute of Geo-environment Monitoring, Professor Qiang Xu and
552 Doctor Guang Zheng of Chengdu University of Technology, Professor Ji Duo and
553 Baoben Xia of Geology and Mineral Resources Exploration Bureau of Xizang
554 Autonomous Region for their participating of our field investigation. We also
555 appreciate the help extended by the Department of Land and Resources of Xizang
556 Autonomous Region and relevant local governments.

557

558 **References**

559 Armijo, R., Tapponnier, P., Mercier, L. and Han, T. L.: Quaternary extension in southern Tibet: Field
560 observation and tectonic implication, *J. Geophys. Research*, **91**(B14),13803-13872, 1986.
561 Armijo, R., Tapponnier, P. and Han, T. L.: Late Cenozoic right-lateral strike-slip faulting in southern

562 Tibet, *J. Geophys. Research*, **94**, 2787-2838, 1989.

563 Avouac, J. P.: Dynamic processes in extensional and compressional settings – mountain building:
564 from earthquakes to geological deformation, *Treatise on Geophys.*, **6**, 377-439, 2007.

565 Bagde, M. N. and Petroš, V.: Fatigue and dynamic energy behaviour of rock subjected to cyclical
566 loading, *Int. J. Rock. Mech. Min.*, **46**, 200–209, 2009.

567 Bettinelli, P., Avouac, J. P. and Flouzat M.: Plate motion of India and interseismic strain in the Nepal
568 Himalaya from GPS and DORIS measurements, *J. Geod.*, **80**, 567–589, DOI
569 10.1007/s00190-006-0030-3, 2006.

570 Bijukchhen S., Takai N., Shigefuji M., Ichiyanaagi M., & Sasatani T. (2017). Strong-Motion
571 Characteristics and Visual Damage Assessment Around Seismic Stations in Kathmandu After
572 the 2015 Gorkha, Nepal, Earthquake. *Earthquake Spectra*, **33**(S1), S219-S242.
573 doi:10.1193/042916EQS074M

574 Bilham, R.: Earthquakes in India and the Himalaya: tectonics, geodesy and history, *Annals*
575 *Geophys.*, **47**(2-3), 839–858, 2004.

576 Chen, Q. Z., Freymueller, J.T., Yang, Z. Q., Xu, C. J., Jiang, W.P., Wang, Q. and Liu, J.N.: Spatially
577 variable extension in southern Tibet based on GPS, *J. Geophys. Research*, **109**, B09401,
578 doi:10.1029/2002JB002350, 2004.

579 Chevalier, M. L., Ryerson, F.J., Tapponnier, P., Finkel, R.C., Jermo, V.D.W., Li, H.B. and Liu, Q.:
580 Slip-Rate measurements on the Karakorum fault may imply secular variations in fault Motion,
581 *Sci.* **307**, 411-414, 2005.

582 China Earthquake Administration: An intensity map of Tibet for the M 8.1 Nepal earthquake.
583 [http://www.cea.gov.cn/publish/dizhenj/468/553/101803/101809/20150501221123458562190/](http://www.cea.gov.cn/publish/dizhenj/468/553/101803/101809/20150501221123458562190/index.html)
584 [index.html](http://www.cea.gov.cn/publish/dizhenj/468/553/101803/101809/20150501221123458562190/index.html), 2015.

585 Cui P., Zhuang, J. Q., Chen, X.C., Zhang, J.Q. and Zhou, X.J.: Characteristics and countermeasures
586 of debris flow in Wenchuan area after the earthquake, *J. Sichuan Univ, (Engineer. Sci. Ed.)*,
587 **42**(5), 10-19, 2010.

588 Dadson, S.J., Hovius, N., Chen, H., Dade, W.B., Lin, J.C., Hsu M.L., Lin, C.W., Horng, M.J., Chen,
589 T.C., Milliman, J. and Stark C.P.: Earthquake-triggered increase in sediment delivery from an
590 active mountain belt, *Geol.*, **32**, 733–736, 2004

591 Dellow, G.D. and Hancox, G.T.: The influence of rainfall on earthquake-induced landslides in New
592 Zealand, in, *Proceed. Tech. Groups, Earthqs. and Urban Develop: New Zealand Geotech. Soc.*
593 *2006 Sym.*, Nelson, New Zealand, 355–368, 2006.

594 Dewey, J., Shackleton, R.M., Chang, C. and Sun Y.: The tectonic evolution of the Tibetan Plateau,
595 *Philos. Trans. R. Soc. London, Ser. A*, **327**, 379-413, 1988.

596 Elliott, J.R., Walters, R.J., England, P.C., Jackson, J.A., Li, Z. and Parsons B.: Extension on the
597 Tibetan plateau: recent normal faulting measured by InSAR and body wave seismology,
598 *Geophys. J. Internat.*, **183**, 503-535. doi: 10.1111/j.1365-246X.2010.04754.x, 2010.

599 GB/T 17742-2008, Standardization Admin. China, 2008.

600 Hovius, N., Meunier, P., Lin, C.W., Chen, H., Chen, Y.G., Dadson, S., Horng, M.J. and Lines M.:
601 Prolonged seismically induced erosion and the mass balance of a large earthquake, *Earth*
602 *Planet. Sc. Lett.*, **304**, 347–355, doi:10.1016/j.epsl.2011.02.005, 2011.

603 Hungr, O., Leroueil, S. and Picarelli L.: The Varnes classification of landslide types, an update,
604 *Landslides*, **11**, 167–194, doi:10.1007/s10346-013-0436-y, 2014.

605 Institute of Geophysics: The M5.9 Tingri earthquake of April 25 2015 in Tibet, *China Earthq.*
606 *Admin.*, <http://www.cea-igp.ac.cn/tpxw/272116.shtml>, 2015.

607 IRIS: Special event: Nepal, *Incorp. Research Insts for Seis*,
608 <http://ds.iris.edu/ds/nodes/dmc/specialevents/2015/04/25/nepal>, 2015.

609 Jouanne, F., Mugnier, J.L., Pandey, M.R., Gamond, J.F., LeFort, P., Serrurier, L., Vigny, C., Avouac
610 J.P. and the Idylhim members: Oblique convergence in the Himalayas of western Nepal
611 deduced from preliminary results of GPS measurements, *Geophys. Research Letts.* **26**,

612 1933–1936. 1999.

613 Larson, K., Burgmann, R., Bilham, R. and Freymueller J.T.: Kinematics of the India-Eurasia
614 collision zone from GPS measurements, *J. Geophys. Res.*, **104**, 1077–1093, 1999.

615 Lave, J., and Avouac J.P.: Active folding of fluvial terraces across the Siwaliks Hills, Himalayas of
616 central Nepal, *J. Geophys. Research*, **105**, 5735–5770, 2000.

617 Li, G., Moelle, K.H.R. and Lewis J.A.: Fatigue crack growth in brittle sandstones, *Int. J. Rock. Mech.*
618 *Min.*, 29, 469–477, 1992.

619 Massey, C.I., Della Pasqua, F., Taig, T., Lukovic, B., Ries, W., Heron, D. and Archibald G.:
620 Canterbury Earthquakes 2010/11 Port Hills Slope Stability: Risk assessment for Redcliffs, *GNS*
621 *Sci.*, Wellington, New Zealand, p. 123 C Appendices, 2014a.

622 Massey, C.I., Taig, T., Della Pasqua, F., Lukovic, B., Ries, W. and Archibald G.: Canterbury
623 Earthquakes 2010/11 Port Hills Slope Stability: Debris avalanche risk assessment for
624 Richmond Hill, *GNS Sci. Consultancy Rept.* 2014/34, 2014b.

625 Molnar, P., and Lyon-Caen H.: Fault plane solutions of earthquakes and active tectonics of the
626 Tibetan Plateau and its margins, *Geophys. J. Internat.*, **99**, 123–153, 1989.

627 Nara, Y., Morimoto, K., Yoneda, T., Hiroyoshi, N. and Kaneko K.: Effects of humidity and
628 temperature on subcritical crack growth in sandstone, *Int. J. Solids Structures*, 48, 1130–1140,
629 2011.

630 Parker, R.N., Hancox, G.T., Petley, D.N., Massey, Densmore, A.L. and Rosser N. J.: Spatial
631 distributions of earthquake-induced landslides and hillslope Preconditioning in the northwest
632 South Island, New Zealand, *Earth forec Dynamics*, 3, (4): 501 DOI: 10.5194/esurf-3-501-2015,
633 2015.

634 Petley, D.N., S.A. Dunning, N.J. Rosser (2005) The analysis of global landslide risk through the
635 creation of a database of worldwide landslide fatalities, in: *Landslide Risk Management*, eds.
636 Hungr, O., R. Fell, R. Couture, E. Eberhardt, Balkema, The Netherlands.

637 Saba, S. B., M. van der Meijde, H. van der Werff (2010). Spatiotemporal landslide detection for the
638 2005 Kashmir earthquake region, *Geomorph.* 124, 17–25,
639 doi:10.1016/j.geomorph.2010.07.026, 2010.

640 Tang, Ch., W-L. Li and J. Ding (2011). Field investigation and research on giant debris flow on
641 august 14, 2010 in Yingxiu town, epicenter of Wenchuan earthquake, *Earth Sci.-J. China Univ.*
642 *Geosci.*, **36**(1), 172-180. doi:10.3799/dqkx.2011.018

643 The Science and Technology Committee and the archives in Xizang Autonomous Region: Tibet
644 earthquakes; historical compilation, (v.1), *People's Publishing House, Xizang*, 1-583, 1982. (in
645 Chinese)

646 USGS: Updated finite fault results for the Apr 25, 2015 Mw 7.9 35 km E of Lamjung, Nepal
647 Earthquake (Version 1), U.S. Geol. Sur., Nat'l. Earthq. Info. Center,
648 <http://earthquake.usgs.gov/earthquakes/eventpage/us20002926#scientific> finite fault, 2015a.

649 USGS: Updated finite fault results for the May 12, 2015 Mw 7.3 22 km SE of Zham, China
650 Earthquake (Version 2), U.S. Geol. Sur. Nat'l Earthq. Info. Center,
651 <http://earthquake.usgs.gov/earthquakes/eventpage/us20002ejl#scientific> finite fault, 2015b.

652 Wang, X.Y. and Han Z.L.: Modeling of landslides hazards induced by the 2008 Wenchuan
653 earthquake using ground motion parameters, in Xie, editor, *Rock stress and earthquakes*,
654 *Taylor & Francis Group*, London, p. 297-304, ISBN 978.0.415.60165.8, 2010.

655 Wu, Z.H., Barosh, P.J., Wu, Z.H., Hu, D.G., Zhan X. and Ye P.S.: Vast early Miocene lakes of the
656 central Tibetan Plateau, *Geol. Soc. Amer., Bull.*, 120, 1326-1337, 2008.

657 Wu, Z.H., Ye, P.S., Barosh P.J. and Wu Z.H.: The October 6, 2008 Mw 6.3 magnitude Damxung
658 earthquake, Yadong-Gulu rift, Tibet, and implications for present-day crustal deformation
659 within Tibet, *J. Asian Earth Sci.*, **40**, (4), 943–957, 2011.

660 Yang, W.T., Wang, M., Kerle, N C., Van Westen, J., Liu, L.Y. and Shi P.J.: Analysis of changes in
661 post-seismic landslide distribution and its effect on building reconstruction, *Nat. Hazards.*
662 *Earth Syst. Sci.*, 15, 817-825. doi:10.5194/nhess-15-817-2015, 2015.

663 Yun S.-H., Hudnut K., Owen S., Webb F., Simons M., Sacco P., Gurrola E., Manipon G, Liang C.,
664 Fielding E., Milillo P., Hua H., & Coletta A. (2015). Rapid Damage Mapping for the 2015Mw
665 7.8 Gorkha Earthquake Using Synthetic Aperture Radar Data from COSMO–SkyMed and
666 ALOS-2 Satellites. *Seismological Research Letters*, 86(6), 1549-1556.
667 doi:10.1785/0220150152

668 Zekkos D., Clark M., Whitworth M., Greenwood W., West A. J., Roback K., Li G, Chamlagain D.,
669 Manousakis J., Quackenbush P., Medwedeff W., & Lynch J. (2017). Observations of
670 Landslides Caused by the April 2015 Gorkha, Nepal, Earthquake Based on Land, UAV, and
671 Satellite Reconnaissance. *Earthquake Spectra*, 33(S1), S95-S114.
672 doi:10.1193/121616EQS237M

673 Zhang, P.Z., Shen, Z.K., Wang, M., Gan, W.J., Burgmann R. and Molnar P.: Continuous
674 deformation of the Tibetan Plateau from global positioning system data, *Geol.*, **32**, 809-812,
675 2004.

676 Zhou, C.C.: Personal communication, November, 2015. *Tibetan Environmental Monitoring Station*,
677 2015.

678

Tables

Table 1 Location of surveyed sites of earthquake intensity in southern Tibet

site	coordinate	intensity	note
Lhasa city	29.65 N, 91.12 E	III	felt area
Xaitongmoin town	29.432 N, 88.259 E	III	felt area
Xigazê city	29.27 N, 88.88 E	IV	felt area
Nâlong city	29.23 N, 91.76 E	IV	felt area
Gamba town	28.276 N, 88.516 E	VI	
Sagya town	28.903 N, 88.020 E	VI	
Lhazê town	29.087 N, 87.634 E	VI	
Ngamring town	29.298 N, 87.234 E	VI	
Sangsang town	29.420 N, 86.724 E	VI	
Saga town	29.329 N, 85.233 E	VI	
Gyirong town	28.856 N, 85.297 E	VI	
Tingri town	28.661 N, 87.122 E	VI	
Dinggyê town	28.367 N, 87.772 E	VI	
Riwu town	28.012 N, 87.681 E	VI	
Rema villiage	28.459 N, 85.224 E	VII	
Bangse villiage	28.083 N, 86.368 E	VII	
Rongxia town	28.057 N, 86.342 E	VII	
Chentang town	27.868 N, 87.414 E	VII	
Natang villiage	27.850 N, 87.441 E	VII	
Jilong town	28.396 N, 85.327 E	VIII	
Sale town	28.365 N, 85.445 E	VIII	
Guoba villiage	28.365 N, 85.457 E	VIII	
Zuobude villiage	28.037 N, 86.297 E	VIII	
Zhangmu town	27.990 N, 85.982 E	IX	
Disgang villiage	27.984 N, 85.979 E	IX	
Lixin villiage	27.960 N, 85.971 E	IX	
Kodari town, Nepal	27.972 N, 85.962 E	IX	
Jifu villiage	28.374 N, 85.329 E	IX	
Chongse villiage	28.373 N, 85.362 E	IX	

Table 2 Distribution of seismic intensity in the southern Tibet region from the Nepal earthquake.

Intensity	Area (km ²)	city, county and town covered by seismic intensity	damage of building and surface
IX	105	The Zhangmu Town of Nyalam County, Jilong Town of Gyirong County.	Most of the mud-brick and stone piled up building were collapsed and severely damaged and some brick houses also have obvious damage and partial collapse. Collapse and landslide is widespread, and the existence of large landslides.
VIII	1,945	The Zhangmu Town and Nyalam Town of Nyalam County, Jilong Town and Sale Town of Gyirong County, Rongxia Town of Tingri County.	Some of the mud-brick and stone piled up buildings were collapsed or severely damaged, but the buildings of brick structure are mainly moderate to slightly damaged and are more of the wall cracks. Medium and small collapses and landslides are common but are rarely large landslide.
VII	9,590	Gyirong County, Nyalam County, Tingri County and Dinggye County.	A few of the mud-brick and stone piled up buildings were severely damaged, but most buildings are slightly damaged only. There are some small collapses, landslides and rockfalls along slope of valley and highway roadcuts.
VI	35,460	Zhongba County, Saga County, Gyirong County, Nyalam County, Tingri County and Dinggye County, Gamba County, Sàgya County, Ngamring County and Lhaz ê	Only a few the mud-brick and stone piled up buildings were slightly damaged, and collapses and landslides are rare. A small amount of rockfall may appear near the highways roadcuts.
Felt area	300,000	Lhasa, Xigaz ê, Burang, Gar and Nêdong etc.	

Figures

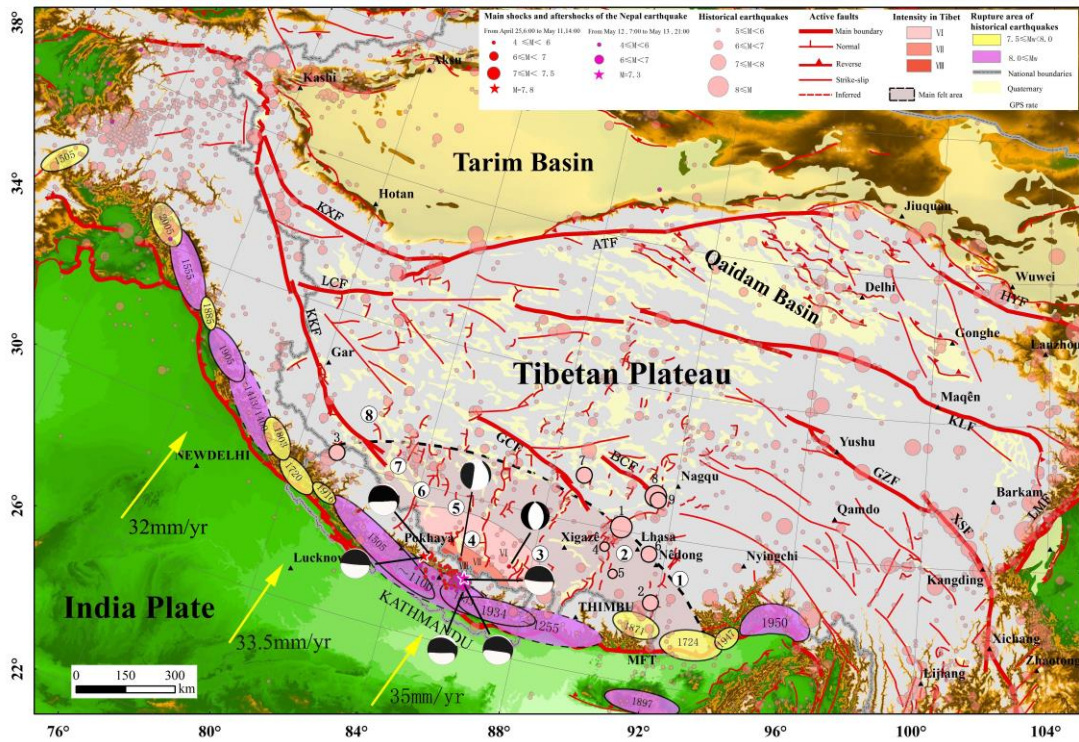


Fig.1 Principal active faults and historic earthquakes in the Himalaya Mountains, Tibetan Plateau and neighboring areas. The earthquake data is from The Science and Technology Committee and the archives in Xizang Autonomous Region, 1982; Bilham, 2004; Avouac, 2007; GPS data from Bettinelli et al, 2006; The focal mechanism solution data from USGS, 2015 a,b and Institute of Geophysics, China Earthquake Administration, 2015. Explanation: Rifts in southern Tibet, ①, Cona-Oiga rift; ②, Yadong-Gulu rift; ③, Dinggye-Xainza rift; ④, Gangga-Tangra Yumco rift; ⑤, Nyalam-Coqân rift; ⑥, Zhongba-Gêzê rift; ⑦, Kunggyu Co-Yagra rift; ⑧, Burang-Gêgyai rift. Thrust and strike-slip faults: MFT, Main Frontal Thrust fault of Himalaya; KKF, Karakorum fault; GCF, Gyaring Co fault; BCF, Beng Co fault; GZF, Ganzi fault; XSF, Xianshuihe fault; KLF, Kunlunshan fault; LMF, Longmenshan fault; LCF, Longmu Co Fault; KXF, Kangxiwa fault; AFT, Altn Tagh fault; HYF, Haiyuan fault. Numbers 1-9, $M \geq 6.8$ historic earthquake epicentral areas in southern Tibet: 1, 1411 M 8.0 Damxung-Yangbajain; 2, 1806 M 7.5 Cona; 3, 1883 M 7.0 Burang; 4, 1901 M 6.8 Nyêno; 5, 1909 M 6.8 Nagarze; 6, 1915 M 7.0 Sangri; 7, 1934 M 7.0 Gomang Co of Xainza; 8, 1951 M

8.0 Beng Co of Nagqu; 9,1952 M 7.5 Gulu of Nagqu.

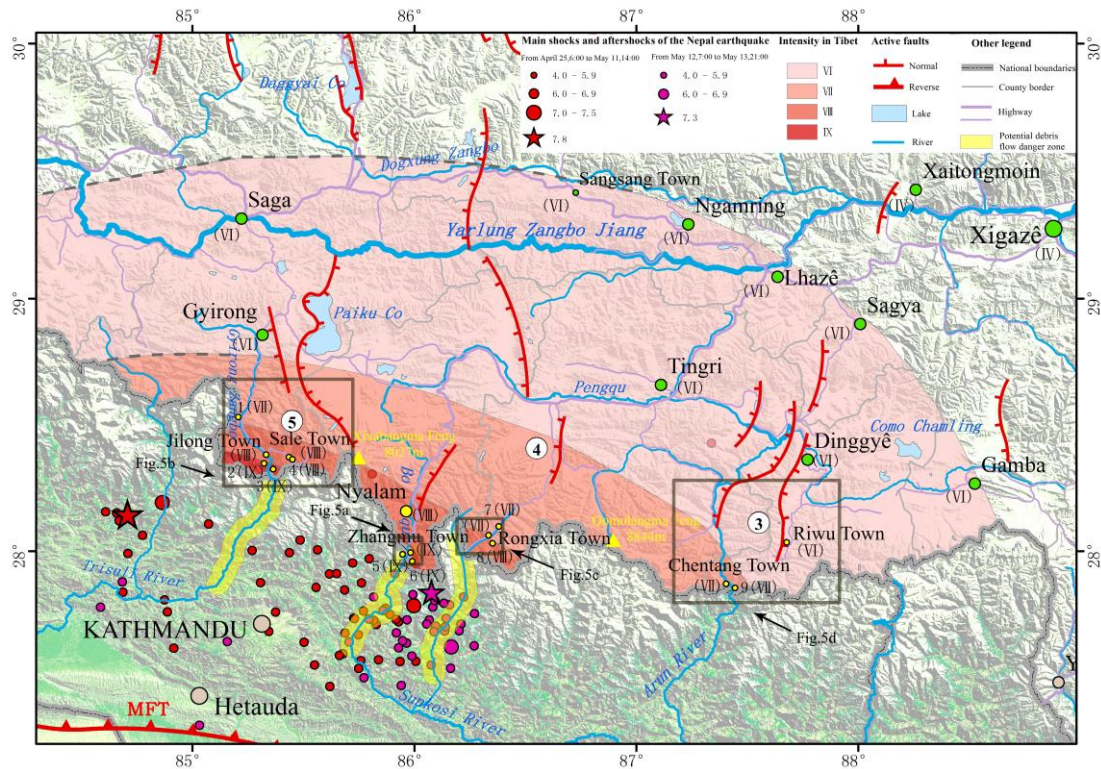


Fig. 2 Principal active faults and the distribution of seismic intensity of the 2015 Nepal earthquake in the southern Tibet region. Epicentral data from the USGS and seismic intensity from the China Earthquake Administration. The numbers and names of the principal S-N trending rifts in southern Tibet are same as on Fig. 1. The green landmarks show the sites which intensity are from China Earthquake Administration, and yellow landmarks show the spots which intensity is resulted from our field investigation. The survey spots: 1, Rema Villiage; 2, Jifu villiage; 3, Chongse Villiage; 4, Guoba Villiage; 5, Kodari Town of Nepal; 6, Lixin Viliage; 7, Bangse Villiage; 8, Zhuobude Villiage; 9, Natang Villiage.



Fig. 3 The building damage resulting at different earthquake intensities: a, Many of the old stone pile or mud-brick houses collapsed, but the new brick houses rarely collapsed at Gangba Village in Sale Town in the intensity VIII zone; b, Similar building damage at Zhuobude Village of Rongxia Town in the intensity VIII zone; c, Most of buildings of brick-concrete structure did not collapse, but many walls showed obvious damage at Nyalam city located in the intensity VIII zone; d, Some walls of the stone-piled or mud-brick houses collapsed at Rema Village, Jilong County, in the intensity VII zone; e, Similar building damage at Chentang Town, Dinggyê county, in the intensity VII zone; f, Most of the houses remain intact and only few or individual walls of buildings had apparent small cracks at Jilong county city in the intensity VI zone.



Fig. 4 Typical earthquake damage in southern Tibet and comparison of houses of different construction (locations shown in Fig. 5). Huge rockfall that smashed the resident committee office building at Disigang Village, about 0.7 km south of Zhangmu, where seven persons were killed (intensity IX) (site 1, Fig. 5a); b, A temporary settlement for earthquake survivors at Jilong; c, Destroyed houses of stone block masonry or adobe construction in Jifu Village southwest of Jilong (intensity VIII) (site 8, Fig. 5b); d, Houses of cement-bonded stone or brick construction in Jifu Village (intensity IX); e, Destroyed old houses and standing new buildings at Sale Town Primary School (intensity VIII) (site 7, Fig. 5b); f, Few collapsed houses at Zhangmu due to the brick structure or reinforced concrete construction (intensity IX).

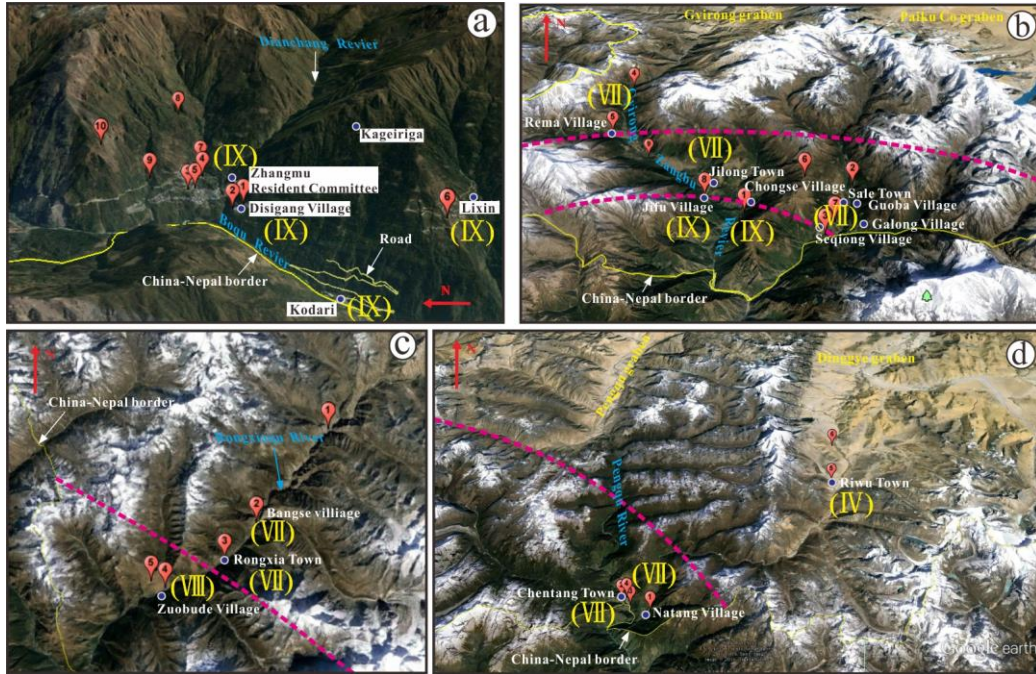


Fig. 5 Main surveyed sites of seismic effects after the Nepal earthquake, see Fig. 2 for the locations (image source Google Earth). Explanation: Roman numerals in brackets, seismic intensity values of the corresponding location; pink dotted lines, boundaries between different intensity zones. a, Zhangmu Town and vicinity; b, Jilong Town and environs; c, Rongxia Town and vicinity; d, Riwu Town to Chentang Town. Explanation: numbered balloons, sites of particular effects; red dashed lines, isoseismal boundaries.



Fig. 6 Geologic effects caused during the Nepal earthquake: a, collapses in the Boqu valley; b, collapse at Disigang Village in the Boqu valley (Site1, Fig. 5a); c. new and old rockfalls at Disigang Village in the Boqu valley (Site1, Fig. 5a); d, destroyed buildings in Kodari, Nepal in the Boqu valley (Site in Fig. 4a); e, large landslide in Chongse Village in the Gyirong Zangbu valley (Site 1, Fig. 5b); f, collapses in Galong Village in the Gyirong Zangbu valley (Site 7, Fig. 5b); g, collapses along highway from Gyirong County to Jilong Town in the Gyirong Zangbu

valley (Site 4, Fig. 5b); h, collapses and fissures along the highway from Jilong to ChongseVillage in the Gyirong Zangbo valley (Site1, Fig. 5b).

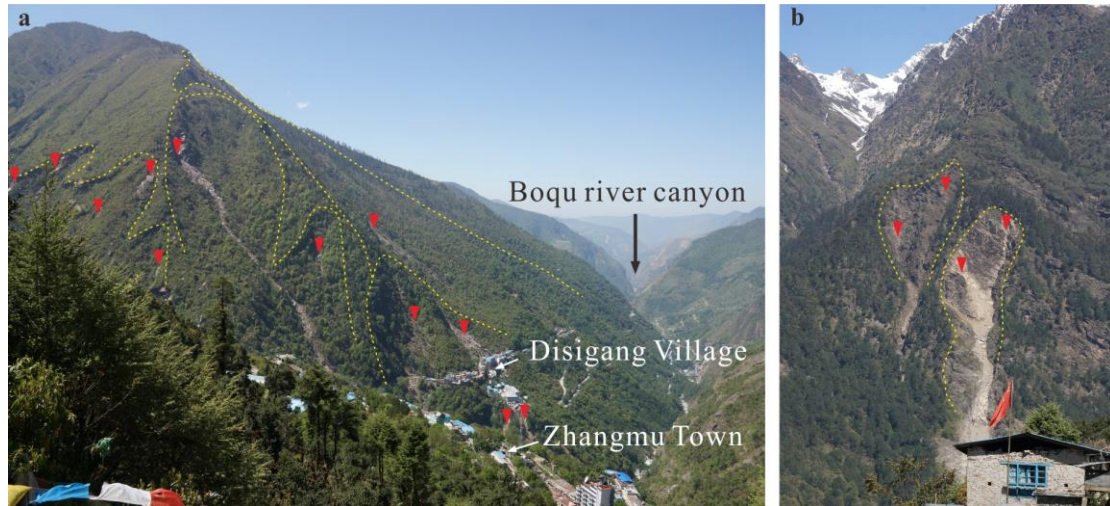


Fig. 7 New and old collapses and landslides on both banks of the Boqu River in Zhangmu Town; a. the east bank; b. the west bank. Explanation: yellow dotted line, boundary of old collapse and landslide; red triangle, new collapse during the Nepal earthquake.



Fig. 8 Fissured and unstable rock masses formed by the earthquake that indicate hazards for additional landslides and rockfalls. Explanation: yellow dotted line, landslide group; arrow, slip direction; red line, new fissures formed during the Nepal earthquake; a, Old landslide group at Zhangmu. b. New fissure in the old landslide group at Zhangmu (site in Fig. 8a); c, Tension fissures at the back edge of Sale Village landslide (site7 in Fig. 5b); d, Dangerous rock mass at Rongxia Primary School (site 3 in Fig. 5c); e, Old landslide with unstable rock at Chentang Town (site 1 in Fig. 5d) and; f, Fissure between unstable rock and bedrock at Chentang (site in Fig. 8e).

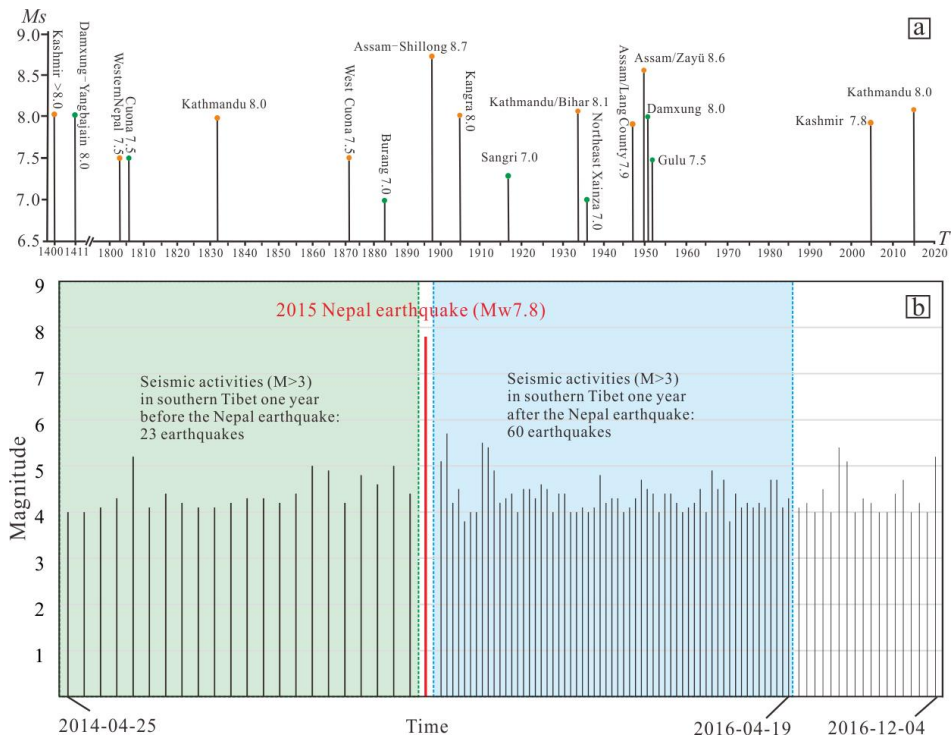


Fig.9 a: Magnitude (M_s) –Time (T) distribution of historical seismic activity along Himalaya and southern Tibet with the magnitude >7.0 . The orange circles show the earthquakes occurred along Himalaya while the green circles show the earthquakes along southern Tibetan rift. b: Magnitude (M) –Time (T) distribution of seismic activity in southern Tibet in the period of one year before and after the 2015 Nepal earthquake (data came from USGS)